NASA Technical Paper 1230

Ferrographic Analysis of Wear Particles From Sliding Elastohydrodynamic Experiments

William R. Jones, Jr., H. S. Nagaraj,
and Ward O. Winer

APRIL 1978

NASA

NASA Technical Paper 1230

Ferrographic Analysis of Wear Particles From Sliding Elastohydrodynamic Experiments

William R. Jones, Jr.
Lewis Research Center, Cleveland, Ohio
H. S. Nagaraj
Mechanical Technology Incorporated, Latham, New York
Ward O. Winer
Georgia Institute of Technology, Atlanta, Georgia

National Aeronautics
and Space Administration

**Scientific and Technical
Information Office**

1978

FERROGRAPHIC ANALYSIS OF WEAR PARTICLES FROM SLIDING ELASTOHYDRODYNAMIC EXPERIMENTS

by William R. Jones, Jr., H. S. Nagaraj,* and Ward O. Winer†

Lewis Research Center

SUMMARY

The Ferrograph was used to analyze oil samples from sliding EHD experiments. Chrome steel balls (AISI 52100) having surface roughnesses of 0.011, 0.076, and 0.38 μm Ra were slid against a sapphire flat. Test conditions included a sliding speed of 1.08 meters per second, a load range of 8.9 to 522 newtons, and a test duration of 25 minutes. Tests were conducted at room temperature (no heat added).

The total amount of wear debris correlated well with average Λ (film thickness to roughness) ratios. The general wear level parameter and the wear severity index yielded similar correlations with average Λ ratios. The generated wear particles were metallic and almost exclusively of the normal rubbing wear type. Similar amounts of wear debris were observed with balls of different surface roughnesses when compared at similar Λ ratios. The Ferrograph was more sensitive in detecting the iron containing wear debris than was the commonly used emission spectrograph (SOAP analysis).

INTRODUCTION

The Ferrograph is an instrument which is capable of magnetically precipitating wear debris from a lubricant onto a glass slide to yield a Ferrogram (refs. 1 to 3). The precipitated particles usually range in size from approximately 0.02 to a few micrometers and are arranged according to size on the slide. The optical density of the deposit on the slide may be measured, and individual particles may be observed with a unique bichromatic microscope, the Ferroscope, or with a scanning electron microscope.

---

*Mechanical Technology Incorporated, Latham, New York.

†Professor of Mechanical Engineering, Georgia Institute of Technology, Atlanta, Georgia.

Elastohydrodynamic lubrication (EHD) refers to the condition of elastically deformed surfaces separated by very thin lubricant films (typically 0.5 to 20 μm thick) (ref. 4). Surface separation is achieved by the generation of high hydrodynamic pressures due to the rapid increase of lubricant viscosity with increasing pressures. Many highly loaded sliding or rolling machine elements with concentrated contact geometries operate in an EHD or partial EHD regime. Ideally, a complete surface separation is effected. However, under conditions of decreasing speed, increasing load, decreasing viscosity, or existence of starvation conditions, surface asperity interactions may occur. As lubricant films become thinner, one may proceed through the following regimes: EHD, partial EHD, boundary, and eventually catastrophic failure.

The objective of this investigation was to use the Ferrograph to determine the relative amount of wear debris and the wear particle types generated by a sliding EHD contact as the film thickness was gradually decreased and asperity interactions began to occur.

Three series of test balls (AISI 52100 steel) were used having surface roughnesses of 0.011, 0.076, and 0.38 micrometer Ra. Experimental conditions included a sliding speed of 1.08 meters per second, a range of loads from 8.9 to 522 newtons (maximum Hz stress range, 0.52 to 2.03 GPa), and a test duration of 25 minutes. Tests were conducted at room temperature (no heat added). The EHD experiments were performed at the Georgia Institute of Technology under NASA grant NGR 11-002-133. The spectrometric oil analyses were performed by Mr. Forrest Handshaw of the Army Oil Analysis Laboratory at Fort Campbell, Kentucky.

A number of commonly used terms are defined in the appendix.

EXPERIMENTAL APPARATUS AND TECHNIQUE

EHD Apparatus

The EHD apparatus (fig. 1) used in this study has been previously reported (refs. 5 to 8). The sliding EHD contact is formed using a 31.8-millimeter-diameter chrome steel (AISI 52100) ball rotating and loaded against a stationary sapphire flat (1.6 mm thick). The temperature of the oil reservoir was monitored with a thermocouple as a function of test time. The oil was not recirculated in these experiments in order to eliminate particle contamination from the recirculation system. A total lubricant charge of 5×10^{-5} cubic meter (50 ml) was used.

Chromium steel balls of three different roughness values were used. The Ra values were 0.011, 0.076, and 0.38 micrometer and will be referred to as smooth (S), medium rough (MR), and rough (R), respectively. These balls were finished by a standard grinding process and did not have any preferred orientation of the surface pattern.

Representative surface profile traces for the three balls and the sapphire flat appear in figure 2. Tests will be referred to as S1, MR1, R1, and so forth, corresponding to the ball roughness and load. Experimental conditions for each test are summarized in table I.

For each test condition film thicknesses were determined by interferometry (ref. 4) at the contact center for the smooth ball. These values were also used for the medium rough and rough ball series. This was necessary because the interference fringes used to measure film thickness disappear as the roughness increases.

The fluid used in this study is a naphthenic mineral oil containing no additives. It has been designated N1 in previous studies (refs. 5 to 8). A complete description of this fluid appears in appendix A of reference 5. A summary of fluid properties appears in table II.

EHD Apparatus Cleaning Procedure

All oil contacting parts were washed with acetone, dried, and rinsed with distilled water. Then all parts were washed with a dilute acid solution. This solution was prepared by adding 10 drops of concentrated nitric acid and 10 drops of concentrated hydrochloric acid to 5×10^{-5} cubic meter (50 ml) of distilled water. This solution dissolved any metallic debris left from the previous test. The parts were then rinsed with distilled sodium bicarbonate solution, distilled water again, and finally with 95 percent ethanol.

Ferrograph

The Ferrograph (refs. 1 to 3) is a commercial instrument used to magnetically precipitate wear particles from a used oil onto a specially prepared glass slide. A mixture of 3×10^{-6} cubic meter (3 ml) of used oil and 1×10^{-6} cubic meter (1 ml) of solvent is prepared. This mixture is then slowly pumped over the slide as shown in figure 3. A washing and drying cycle follows which removes residual oil and permanently attaches the particles to the slide. The resulting slide with its associated particles is called a Ferrogram.

The amount of wear debris on a Ferrogram can be determined by measuring the optical density of the deposit at various positions along the slide. The readings are expressed as the percent area covered by the particles in a field of view of 1.2 millimeter diameter. In this way, a composite Ferrogram density can be determined for each set of conditions.

Ferrogram slides are approximately 60 millimeters long. As shown in figure 3, the oil sample first contacts the slide at a position 55 or 56 millimeters from one end. This area is designated as the entry position. In principle, the larger wear particles will appear in this region. As the oil traverses the slide, there is a gradual gradation in particle size. The smallest particles will then appear in the exit region which is about 10 millimeters from the end of the slide. This gradation in particle size as a function of Ferrogram position is illustrated in figure 4.

Optical density measurements were made on each Ferrogram at several different locations: entry, 54, 50, 40, 30, 20, and 10 millimeters. In addition a composite or representative density was determined by averaging these seven readings. A density reading of less than 1 percent was treated as a zero. Optical density measurements for all tests appear in table III.

RESULTS AND DISCUSSION

Ferrogram Results

Photomicrographs of the Ferrogram entry region for each of the tests with the smooth, medium rough, and rough ball series appear in figures 5 to 7, respectively. The general trend of increasing wear particle density with increasing load (or decreasing film thickness) is evident. In one test (S2), the observation of nonmetallic debris or large oxide flakes, which were unrelated to the wear process, caused a high optical density reading.

Often pile-ups of both metallic and nonmetallic debris occur at the entry position. Since this makes it difficult to assess the wear level, an alternate procedure is to examine the debris at a location some distance from the entry. Typically this is the 54-millimeter position. Micrographs taken at this location for all tests appear in figures 8 to 10. Again, the trend of the increasing amounts of wear debris with increasing load in both the medium rough and rough ball series is obvious. However, most of the particles present at the 54-millimeter position in the smooth series are not wear related. These particles are transparent and nonmetallic.

Wear as a Function of Λ Ratio

A convenient parameter for predicting the degree of surface interactions is the ratio of the central film thickness to the composite surface roughness. This dimensionless parameter Λ is mathematically defined as

$$\Lambda = \frac{h_0}{\left(\sigma_1^2 + \sigma_2^2\right)^{1/2}} \tag{1}$$

where h_0 is the central film thickness and σ_1 and σ_2 are the Ra surface roughnesses of the two contacting surfaces. In this study, the two surfaces were the sapphire disk and steel ball. Since bath temperature was changing during the tests (and thus h_0), an average $\Lambda(\Lambda_{avg})$ was calculated for each test and appears in table I.

A plot of composite Ferrogram density for each test as a function of Λ_{avg} appears in figure 11. The large and very rapid increase in particle density at low Λ values is evident. The transition to the high wear regime occurs as the Λ ratio approaches 1. This is in agreement with the findings of other investigators. Tallian (ref. 9) has shown that the onset of surface distress occurs at a Λ value of about 1.5. Czichos (ref. 10) reports that the change from a full EHD film to continuous asperity contact occurs as Λ decreases from 2.5 to 0.8. In figure 11, at Λ values greater than 1, a composite particle density of between 1 and 2 percent is observed. Since a full film should be present at these higher Λ ratios, little wear should take place. Therefore, these density readings represent the background or contaminant particle density for this set of experiments.

As shown in table I, there was an overlap of Λ values in each test series. There were four sets of tests that yield similar average Λ ratios. These were S3-MR1, S4-S5-MR2, MR3-R1, and MR4-R2. One would expect the generation of a similar amount of debris under these similar Λ ratios. The composite Ferrogram densities for these four sets of experiments appear in figure 12 and a good correlation is observed.

General Wear Level Parameter and Wear Severity Index

Other wear parameters can be determined from optical density measurements. Two parameters that are advocated by Bowen and Westcott (ref. 11) are the general wear level parameter, $A_L + A_S$ and the wear severity index, $A_L^2 - A_S^2$. A_L and A_S are the optical density readings (percent area covered) on the Ferrogram where large and small particles are precipitated, respectively. Typically, A_L is taken at the entry and A_S at the 50-millimeter position.

For normal wear processes, A_L is usually slightly greater than A_S. However, if an abnormal wear process occurs, A_L will be much larger than A_S. Therefore, $A_L + A_S$ yields the general level of wear, while $A_L - A_S$ gives an indication of abnormality. These two parameters may be multiplied together $(A_L + A_S)(A_L - A_S)$, to produce the wear severity index, $A_L^2 - A_S^2$. This latter parameter is quite sensitive to the onset of severe wear.

For this study, the general wear level parameter and the wear severity index are tabulated in table IV and plotted as a function of Λ_{avg} in figures 13 and 14. Both parameters exhibit large increases at low Λ_{avg} values. As expected, these trends are similar to that observed in figure 11, composite Ferrogram density as a function of Λ_{avg}.

Λ Variations as a Function of Test Time

In the normal operation of the EHD apparatus, the lubricant is circulated through a heat exchanger to maintain a constant bath temperature. During preliminary experiments, it was found that a great deal of extraneous debris was introduced into the oil from the recirculation system. This extraneous debris made it difficult to interpret the Ferrogram results. Therefore the heat exchanger was not utilized in these studies, and no attempt was made to control the oil bath temperature. The bath temperatures were monitored during the course of each experiment and are tabulated in table V.

Obviously, as the bath temperature rises there will be a corresponding decrease in viscosity and therefore in the film thickness and Λ. Values of Λ were calculated for each test and bath temperature appearing in table V. All the Λ ratios at test conclusion were lower than the initial Λ value. However, only in tests S4, S5, and MR3, did the Λ ratios approach or drop below the transition value of 1. The final Λ ratios for S4, S5, and MR3 were 1, 1, and 0.5, respectively, and these values were reached only in the last few minutes of the test. Tests having initial Λ ratios greater than 3 yielded final Λ values greater than 1.5. All other tests have initial Λ values already below 1. Therefore, a linear average of the ratios was calculated for each test and used for the various correlations. These values (Λ_{avg}) appear in table I.

In five of the tests (MR3 and MR4, R2, R3, and R4) which yielded appreciable wear, there was a decrease (<30%) in ball surface roughness measured at test conclusion. This run-in effect has been noted by others (ref. 10). This change in surface roughness was not taken into account in the Λ calculations. Values of Λ_{avg} for these five tests were already below the transition value of 1.

Effect of Ra Measurement on Λ Ratio

The Ra value for a surface depends on the wavelength range of the particular type of profilometer used. Recent studies (ref. 12) on asperity interactions inferred from infrared temperature measurements indicate that the Ra value used to calculate Λ should consider only wavelengths in the range $d/4 \leq \lambda \leq 2d$, where d is the Hertzian contact diameter. The profilometer used in this study had a fixed wavelength range of

0.76 millimeter to 13 micrometers. The upper limit was set through electrical filtering while the lower limit was determined by the stylus radius. Slightly different Λ ratios would have resulted if the wavelength range d/4 to 2d had been used in determining Ra for each of the load conditions (and thus a different d) of this study. However, the basic conclusions of these experiments would not be altered.

Wear Particle Morphology

Microscopic examination of the wear debris yielded the following information. Essentially, all of the metallic wear particles, regardless of the initial surface roughness, were of the "normal rubbing wear" variety. That is, they were composed of small asymmetric thin (metallic) flakes. These flakes were typically less than 10 micrometers in major dimension and no more than 1.5 micrometers thick. On the Ferrograms, these particles are typically arranged in strings because of the magnetic field generated by the Ferrograph. An example of this type of debris from test R4 is shown in figure 15.

Two of the tests, MR4 and R4, yielded a second wear particle type. Typically, these particles were large bright flakes 20 to 60 micrometers in major dimension and <3 micrometers thick. An example of this particle type (from test R4) is shown in figure 16. They were located at random on the Ferrograms and were not normally alined with the magnetic field. This behavior on the Ferrograms indicated that they were nonferrous and most likely aluminum. Heating the Ferrograms containing these particles to 330° C for 90 seconds caused the steel rubbing wear particles to change to a characteristic blue color. The blue color is caused by interference effects due to surface oxidation. The large flakes became bright silvery white confirming that they were aluminum. No doubt, there was a connection between the appearance of the large aluminum particles and the failure of the driving collar adhesive which occurred on tests MR4 and R4. This failure would cause the rotating drive shaft to touch the aluminum housing thus producing aluminum wear particles. This particle type was not observed in any other oil samples.

Wear Regimes

A number of investigators have classified the various wear regimes that occur in sliding contacts. Reda, et al. (ref. 13) have identified six different wear regimes occurring at the interface between sliding steel surfaces. Each regime produces characteristic wear particles.

In regime 1 a full EHD film is normally present, wear rates are very low, and therefore few wear particles are observed. The wear particles that are observed are

normally generated during startup or shutdown where some metallic contact does occur. Typically, these particles are free metal of the normal rubbing wear type having major dimensions of less than 5 micrometers. Obviously, this regime corresponds to most tests of the present study where the Λ ratio is greater than 1.

Regime 2 refers to the normal boundary lubrication mode where there is a continuous generation of normal rubbing wear particles. These particles are free metal, less than 15 micrometers in major dimension and less than 1 micrometer thick. The rest of the tests from the present study fall into this regime where the Λ ratio is less than 1.

In regime 3, a breakdown of the boundary lubricant film occurs. The wear rate is high and the wear particles are free metal ranging in size from submicron to 150 micrometers. Regimes 4 and 5 are normally observed under unlubricated conditions and therefore do not really apply to this study. Regime 6 refers to the condition of catastrophic surface failure resulting in free metal wear particles up to 1 millimeter. Obviously, regimes 3 and 6 were not observed in these studies.

Spectrometric Oil Analysis Results

A commonly used analytical method to determine the elemental concentrations of debris in a used oil is spectrometric analysis, commonly referred to as SOAP. An emission spectrograph was used to analyze each oil sample from this study. An unused oil sample was also tested as a blank. The blank contained small concentrations of a variety of different elements, but no iron or aluminum was detected. These elemental concentrations from the blank were then subtracted from all other readings. Results for the three elements (Fe, Al, and Cr) that could conceivably be related to the materials of the test rig appear in table VI.

It is obvious from table VI that most of the samples were barely within the limits of detection for the emission spectrograph. Little iron-containing wear debris was detected until the relatively high wear situation of the rough ball series was reached. However, even at the highest wear condition, R4, which had a composite Ferrogram density of 26.9, the spectrograph only detected 4 ppm of iron. This indicates that, for detecting the iron-containing wear debris from these studies, the Ferrograph is more sensitive than the normal SOAP procedures.

The chromium present in the oil samples probably reflects the background variation in the blank. Chromium is present in the 52100 steel but it is at too low a concentration (1.5 percent) to be detected in these experiments. The aluminum in sample R4 is, no doubt, related to the driving collar failure. Its presence was discussed earlier. Sample S2 contained a large amount of extraneous debris which is reflected in the SOAP results as well as the Ferrogram densities.

Correlation of SOAP and Ferrogram Densities

After comparing the SOAP and Ferrograph results, there was a possibility that the spectrograph might not be "seeing" all of the wear particles. This could be caused by a particle settling problem or a number of other factors. Therefore, in an attempt to correlate the results from the two techniques, the following assumptions were made. The average dimensions of the Ferrogram deposits (assumed to be all Fe) were: 50 millimeters long by 0.10 millimeter wide by 1.5 micrometer thick. Then for complete coverage (100 percent density reading), this corresponds to a particle volume of 7.5×10^{-3} mm^3. With a specific gravity of 8, the total mass of the deposit would be about 60 micrograms. Since approximately 3 grams of oil are passed over each Ferrogram, 60 micrograms of wear debris would represent about 20 ppm by weight. Multiplying the fractional optical densities of the rough ball series times 20 results in the following Fe concentrations: R1 - 0.4 ppm, R2 - 1 ppm, R3 - 4 ppm, and R4 - 5 ppm. Therefore, the SOAP results (Fe concentrations) are consistent with the values obtained with the Ferrograph.

This is in contrast to data reported by Ruff (ref. 14) in which analytical Fe standards were analyzed by Ferrography and a spectrometric method. The spectrometric results yielded Fe concentrations 50 percent too high, while the Ferrograph values were 50 percent too low. The high SOAP reading was not explained but the low Ferrograph result was attributed to the size distribution of the wear debris. Apparently, much of the iron content consisted of very small particles which could not be magnetically recovered or of a dissolved species. Obviously this was not the case in the present study.

In these experiments only five samples (MR4, R1, R2, R3, and R4) yielded appreciable metallic entry deposits. Pocock and Gadd (ref. 15) have shown a correlation between the product of the height of the entry deposit h and the percent area covered at the entry P with the amount of iron in the oil sample. A similar plot for the above five samples is shown in figure 17. A correlation also appears to exist here. The Pocock and Gadd data is shown for comparison, even though the exact volume of oil passed over the Ferrogram was not stated.

Friction Coefficients

Average friction coefficients for comparable tests measured at a steady state bath temperature of 40° C appear in figure 18. As one would expect, fairly constant values (0.061 to 0.062) were observed for all tests at average Λ ratios greater than 1.5 where a full EHD film existed. As Λ_{avg} decreased below 1 and asperity interactions increased, the friction values also increased, as expected. No abrupt friction increases or transitions were observed which would have signaled a boundary film failure or a

catastrophic failure mode. This agrees with the wear particle analysis previously discussed.

SUMMARY OF RESULTS

The Ferrograph was used to analyze oil samples from sliding EHD experiments. Chrome steel balls (AISI 52100) having surface roughnesses of 0.011, 0.076, and 0.38 μm Ra were slid against a sapphire flat. Test conditions included a sliding speed of 1.08 meters per second, a load range of 8.9 to 522 newtons, and a test duration of 25 minutes. Tests were conducted at room temperature (no heat added). The major results were as follows:

1. The relative amount of wear debris correlated well with average Λ (film thickness to roughness) ratios. Much debris was observed at Λ values <1, little debris at Λ's > 1.

2. The general wear level parameter and the wear severity index yielded similar correlations with average Λ ratios.

3. The wear particles that were generated were metallic and almost exclusively of the normal rubbing wear type. No catastrophic failure modes were experienced.

4. Similar amounts of wear debris were observed with balls of different surface roughnesses when compared at similar Λ ratios.

5. The Ferrograph was more sensitive in detecting the iron containing wear debris than was the commonly used emission spectrograph (SOAP analysis).

Lewis Research Center,
National Aeronautics and Space Administration,
Cleveland, Ohio, February 21, 1978,
505-04.

APPENDIX - GLOSSARY

Ferrogram - a glass slide onto which wear debris is deposited using the Ferrograph

Ferrograph - a device which uses a magnetic principle to precipitate wear debris onto a glass slide from an oil sample

General Wear Level Parameter ($A_L + A_S$) - sum of the optical density readings for large and small wear particles on a Ferrogram. This parameter indicates the level of wear

Lambda Ratio (Λ) - ratio of the central oil film thickness to the composite surface roughness

Normal Rubbing Wear Particles - small metallic flakes which result from sliding wear processes

SOAP Analysis - elemental analysis of oil samples using an emission spectrograph

Wear Severity Index $\left(A_L^2 - A_S^2\right)$ - difference between the squares of the optical density readings for the large and small wear particles on a Ferrogram. This parameter indicates the onset of severe wear

REFERENCES

1. Seifert, W. W.; and Westcott, V. C.: A Method for the Study of Wear Particles in Lubricating Oil. Wear, vol. 21, 1972, pp. 27-42.

2. Westcott, V. C.; and Seifert, W. W.: Investigation of Iron Content of Lubricating Oil Using Ferrograph and an Emission Spectrometer. Wear, vol. 23, 1973, pp. 239-249.

3. Scott, D.; Seifert, W. W.; and Westcott, V. C.: Ferrography - An Advanced Design Aid for the 80's. Wear, vol. 34, 1975, pp. 251-260.

4. Wedeven, Lavern D.: What is EHD? Lubr. Eng., vol. 31, no. 6, June 1975, pp. 291-296.

5. Sanborn, D. M.; and Winer, W. O.: Fluid Rheological Effects in Sliding Elastohydrodynamic Point Contacts with Transient Loading: I - Film Thickness. J. Lubr. Technol., vol. 93, Apr. 1971, pp. 262-271.

6. Turchina, V.; Sanborn, D. M.; and Winer, W. O.: Temperature Measurements in Sliding Elastrohydrodynamic Point Contacts. J. Lubr. Tech., vol. 96, July 1974, pp. 464-471.

7. Ausherman, V. K.; et al.: Infrared Temperature Mapping in Elastohydrodynamic Lubrication. J. Lubr. Tech., vol. 98, 1976, pp. 236-243.

8. Nagaraj, H. S.; Sanborn, D. M.; and Winer, W. O.: Effects of Load, Speed, and Surface Roughness on Sliding EHD Contact Temperatures. J. Lubr. Tech., vol. 99, 1977, pp. 254-263.

9. Tallian, T. E.: On Competing Failure Modes in Rolling Contact. ASLE Trans., vol. 10, 1967, pp. 418-439.

10. Czichos, Horst: Influence of Asperity Contact Conditions on the Failure of Sliding Elastohydrodynamic Contacts. Wear, vol. 41, 1977, pp. 1-14.

11. Bowen, E. Roderic; and Westcott, Vernon C.: Wear Particle Atlas. Naval Air Engineering Center, Lakehurst, N.J., July 1976.

12. Winer, Ward O.; and Sanborn, David M.: Lubricant Rheology Applied to Elastohydrodynamic Lubrication. NASA CR 2837, 1977.

13. Reda, A. A.; Bowen, R.; and Westcott, V. C.: Characteristics of Particles Generated at the Interface Between Sliding Steel Surfaces. Wear, vol. 34, 1975, pp. 261-273.

14. Ruff, A. W.: Study of Initial Stages of Wear by Electron Channeling. II: Quantitative Methods in Wear Debris Analysis. National Bureau Standards, NBSIR-76-1141, 1976.

15. Pocock, G.; and Gadd, P.: The Relationship Between the Ferrogram Entry Deposit and the Iron Content of Used Lubricating Oils. Wear, vol. 39, 1976, pp. 161-165.

TABLE I. - EXPERIMENTAL TEST CONDITIONS

[Sliding speed for all tests was 1.08 m/sec.]

Test	Load, N	Maximum Hertz stress, GPa	Average Λ ratio, Λ_{avg}
S1	8.9	0.52	22
S2	67	1.0	10
S3	215	1.5	4.6
S4	307	1.7	1.8
S5	522	2.0	1.5
MR1	8.9	0.52	4.3
MR2	67	1.0	2.0
MR3	215	1.5	.8
MR4	307	1.7	.2
R1	8.9	0.52	0.9
R2	67	1.0	.4
R3	215	1.5	.1
R4	307	1.7	$<.1$

TABLE II. - TEST FLUID PROPERTIES

Chemical type	Naphthenic mineral oil
Absolute viscosity, 38° C, N-sec/m^2 (cP)	2.18×10^{-2} (21.8)
Absolute viscosity, 99° C, N-sec/m^2 (cP)	3.2×10^{-3} (3.2)
Atmospheric pressure viscosity coefficient, $(N/m^2)^{-1}$	2.22×10^{-8}
Density, 38° C, g/ml	0.904
Density, 99° C, g/ml	0.866
Pour point, °C	-43
Flash point, °C	157
Fire point, °C	185
Average molecular weight	305

TABLE III. - OPTICAL DENSITY OF FERROGRAMS AT VARIOUS FERROGRAM POSITIONS

Sample	Optical density at various positions on Ferrogram, percent area covered							Composite density
	Entry	54	50	40	30	20	10	
S1	<1	<1	1.2	<1	<1	<1	<1	0.2
[a]S2	15.3	4.4	1.0	1.9	1.3	1.8	<1	3.7
S3	4.2	4.3	<1	<1	<1	1.5	<1	1.4
S4	3.1	<1	<1	<1	<1	<1	<1	.4
S5	7.1	<1	<1	1.2	<1	<1	<1	1.2
MR1	1.6	1.8	1.8	<1	<1	4.1	2.6	1.7
MR2	3.7	1.6	1.2	<1	1.0	1.8	1.5	1.5
MR3	5.3	2.3	2.0	<1	<1	1.5	1.7	1.8
MR4	19.8	5.8	4.3	3.3	4.0	4.0	3.7	6.4
R1	7.1	2.0	1.0	1.4	<1	1.3	<1	1.8
R2	21.3	9.4	5.4	5.0	2.8	2.4	1.0	6.7
R3	36.9	24.6	19.6	14.0	10.4	11.7	14.0	18.7
R4	40.6	39.5	28.8	24.8	23.4	16.0	15.4	26.9

[a]Large amount of nonmetallic debris.

TABLE IV. - GENERAL WEAR LEVEL PARAMETER

$(A_L + A_S)$ AND WEAR SEVERITY INDEX $\left(A_L^2 - A_S^2\right)$

Test	General wear level parameter, $A_L + A_S$	Wear severity index, $A_L^2 - A_S^2$
S1	1.2	0
S2	16.3	233
S3	4.2	17.6
S4	3.1	9.6
S5	7.1	50.4
MR1	3.4	0
MR2	4.9	12.4
MR3	7.3	24.1
MR4	24.1	374
R1	8.1	49.4
R2	26.7	425
R3	56.5	976
R4	69.4	819

TABLE V. - OIL BATH TEMPERATURES (°C)

AT VARIOUS TEST TIMES

Sample	Time, min									
	0	3	6	9	12	15	18	21	24	25
S1	25.5	26	26.3	26.6	26.9	27.2	27.5	27.7	27.8	27.8
S2	25.5	28.5	31.5	32.5	34	35.5	37	38	39.1	39.5
S3	24.5	33.5	38.5	43.7	48.2	52.3	57	58.9	62	63
S4	23.5	30.3	35.7	40	44	47	50.5	54	57.3	58.5
S5	26	32.5	36.9	40.2	43.2	46.1	48.7	51	53.5	54.3
MR1	23.5	23.9	24.4	24.8	25.1	25.4	25.7	25.9	26.1	26.2
MR2	22.3	26.7	29.1	31.1	32.9	34.4	35.9	37.4	38.6	39.0
MR3	23.8	35.8	43.3	50	56.7	61.5	64.6	68.1	72	73.2
MR4	25.2	41.7	55.5	62.8	70.5	76.5	82.3	85.4	(a)	----
R1	25	25.6	26.3	26.8	27.2	27.6	28	28.4	28.7	28.8
R2	24.9	30.3	33.7	36.3	38.3	40.1	41.9	43.4	44.8	45.2
R3	25	42.7	52.3	59.3	65.3	71	75.6	80.3	84.2	85.5
R4	22.1	43.2	57.3	65.7	73.3	80	86.4	92.1	(a)	----

[a]Tests terminated at 23 min due to failure of adhesive on driving collars.

TABLE VI. - SPECTROGRAPHIC

ANALYSIS OF OIL SAMPLES

Sample	Element concentration, ppm		
	Fe	Al	Cr
S1	-	-	-
S2	1	2	1
S3	1	-	-
S4	1	-	-
S5	-	-	1
MR1	-	-	-
MR2	1	-	-
MR3	1	-	-
MR4	1	-	1
R1	-	-	-
R2	2	-	-
R3	3	-	-
R4	4	3	-

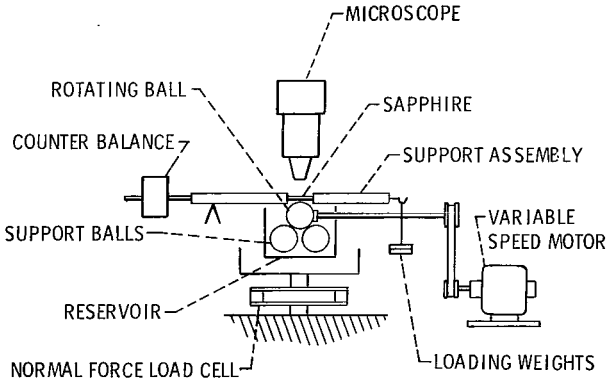

Figure 1. - Sliding EHD apparatus.

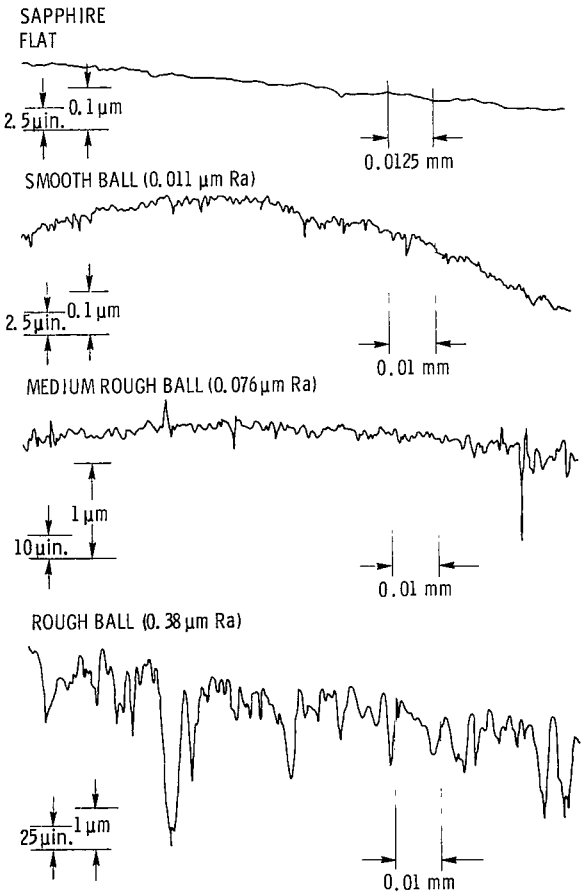

Figure 2. - Representative surface roughness profiles for the three test balls and sapphire flat.

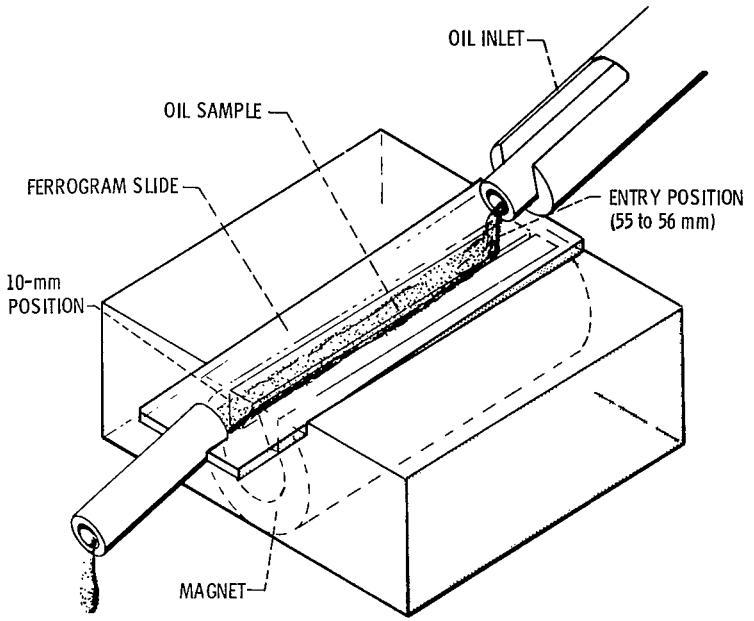

Figure 3. - Ferrograph analyzer.

(a) Entry.

(b) 54.0 millimeters.

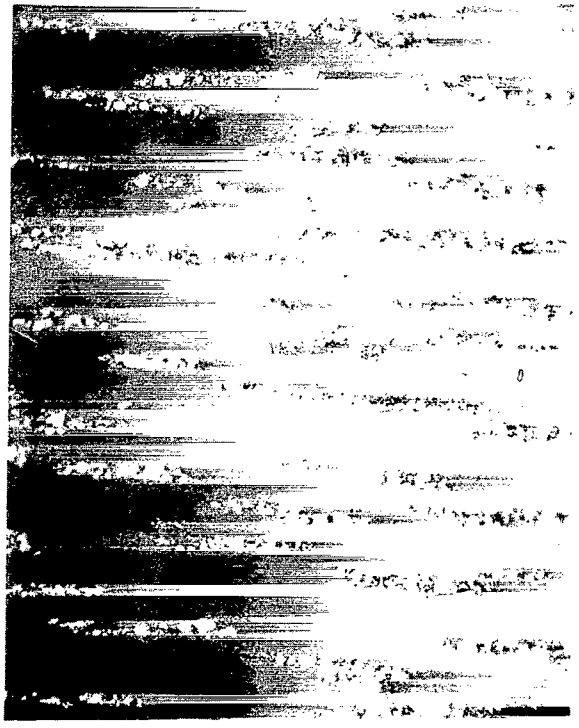

(c) 50.0 millimeters.

(d) 10.0 millimeters.

Figure 4. - Wear debris at various Ferrogram locations for test R3 ($\Lambda_{avg} = 0.1$).

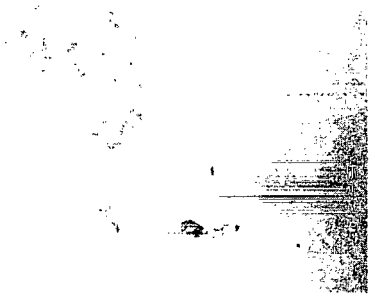

(a) S1 ($\Lambda_{avg} = 22$).

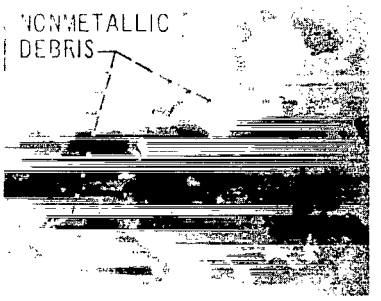

(b) S2 ($\Lambda_{avg} = 10$).

(c) S3 ($\Lambda_{avg} = 4.6$).

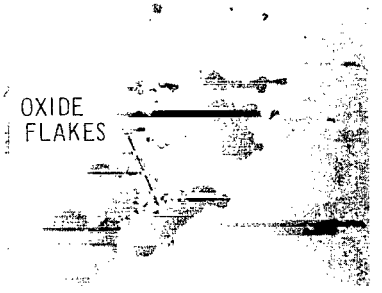

(d) S4 ($\Lambda_{avg} = 1.8$).

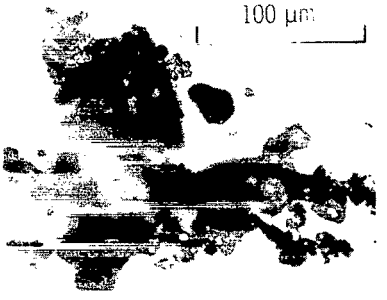

(e) S5 ($\Lambda_{avg} = 1.5$).

Figure 5. - Ferrogram entry deposit for smooth ball series.

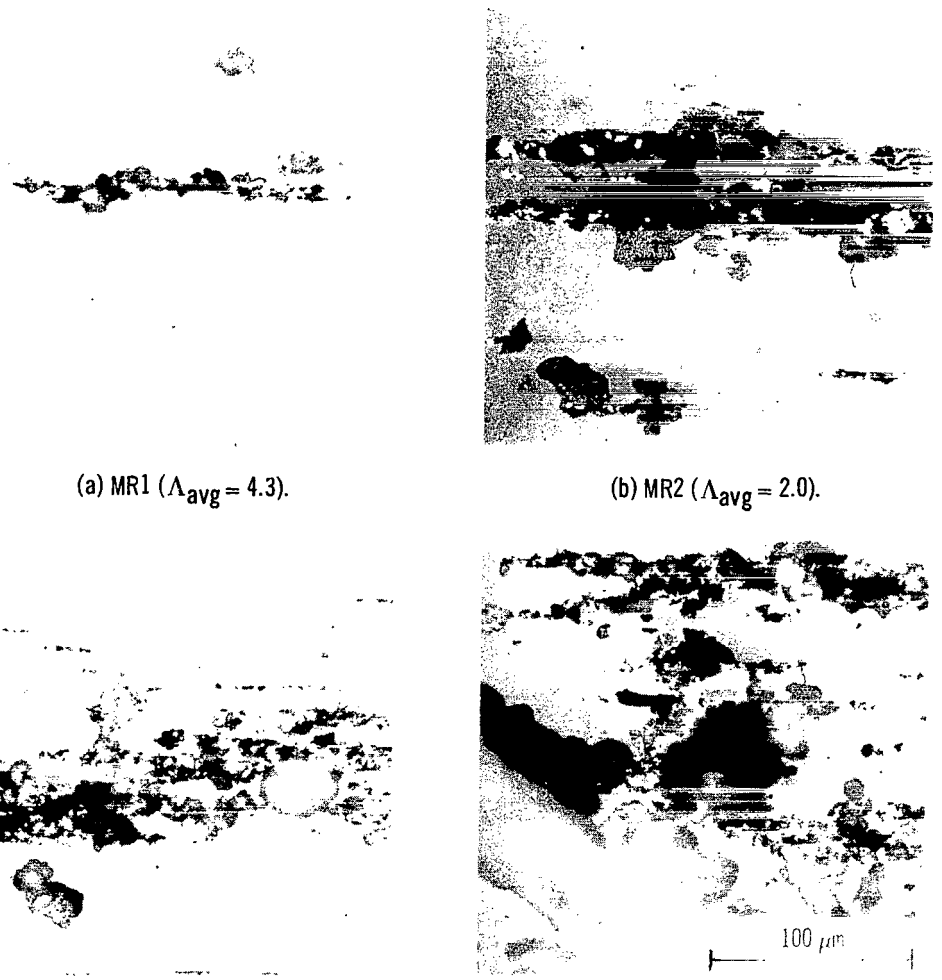

(a) MR1 ($\Lambda_{avg} = 4.3$).

(b) MR2 ($\Lambda_{avg} = 2.0$).

(c) MR3 ($\Lambda_{avg} = 0.8$).

(d) MR4 ($\Lambda_{avg} = 0.2$).

Figure 6. - Ferrogram entry deposit for medium rough ball series.

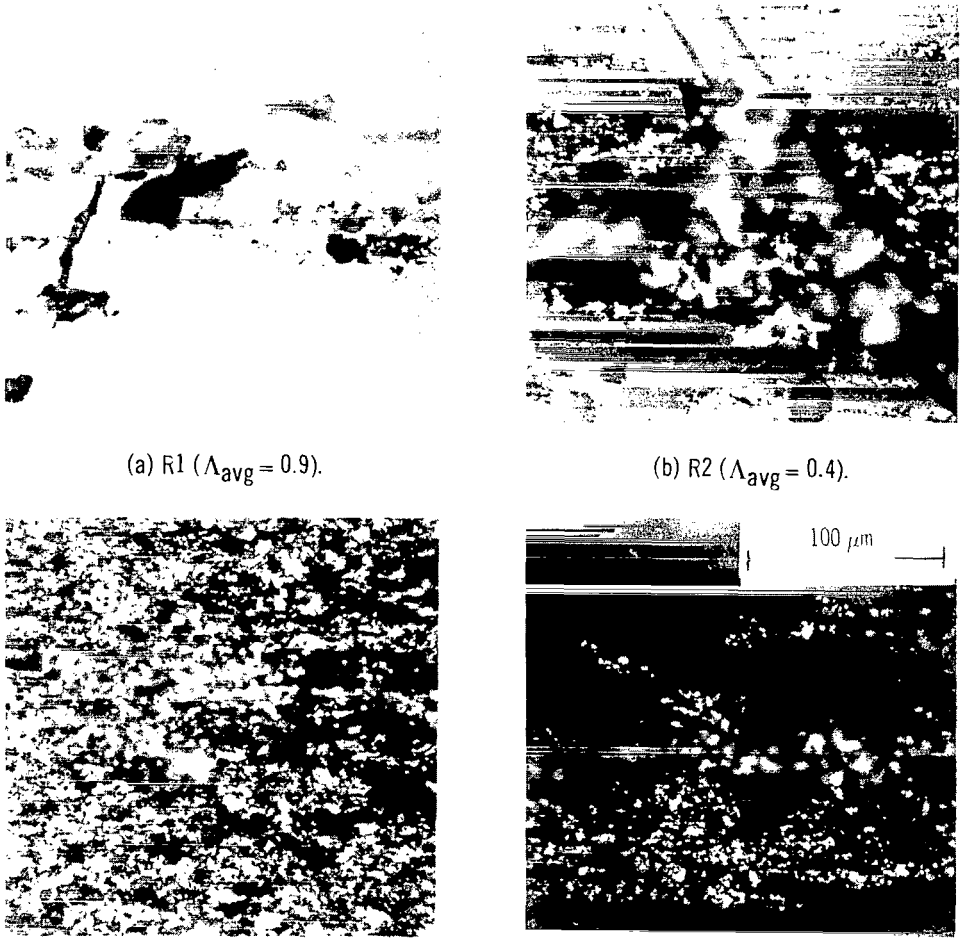

(a) R1 ($\Lambda_{avg} = 0.9$).

(b) R2 ($\Lambda_{avg} = 0.4$).

(c) R3 ($\Lambda_{avg} = 0.1$).

(d) R4 ($\Lambda_{avg} < 0.1$).

Figure 7. - Ferrogram entry deposit for rough ball series.

(a) S1 ($\Lambda_{avg} = 22$).

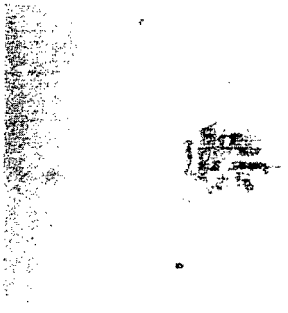

(b) S2 ($\Lambda_{avg} = 10$).

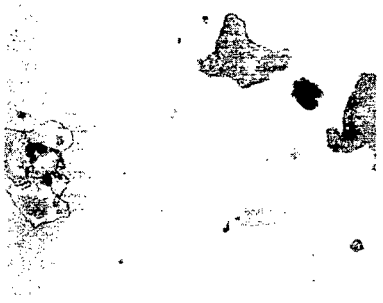

(c) S3 ($\Lambda_{avg} = 4.6$).

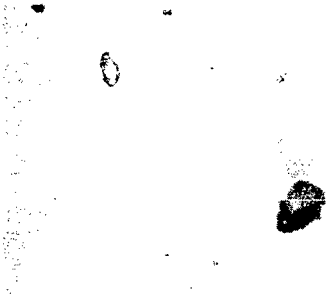

(d) S4 ($\Lambda_{avg} = 1.8$).

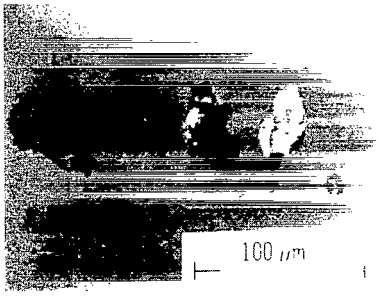

(e) S5 ($\Lambda_{avg} = 1.5$).

Figure 8. - Ferrogram deposit at 54 millimeters for smooth ball series.

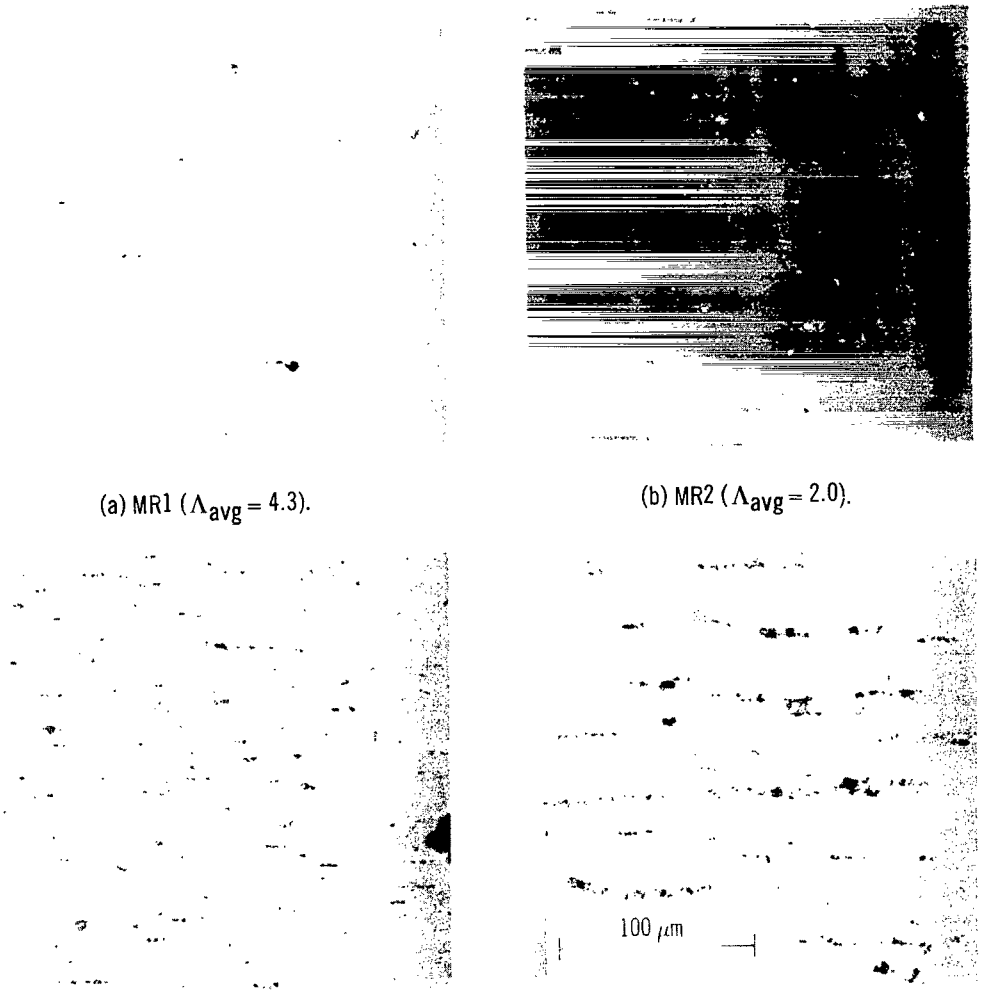

(a) MR1 ($\Lambda_{avg} = 4.3$).

(b) MR2 ($\Lambda_{avg} = 2.0$).

(c) MR3 ($\Lambda_{avg} = 0.8$).

(d) MR4 ($\Lambda_{avg} = 0.2$).

Figure 9. - Ferrogram deposit at 54 millimeters for medium rough ball series.

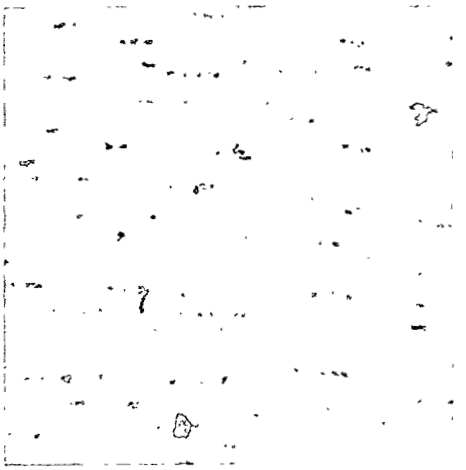

(a) R1 ($\Lambda_{avg} = 0.9$).

(b) R2 ($\Lambda_{avg} = 0.4$).

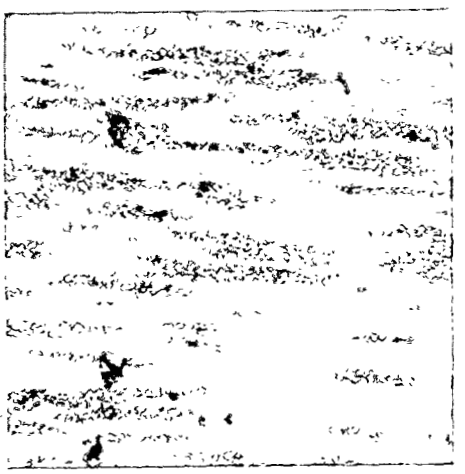

(c) R3 ($\Lambda_{avg} = 0.1$).

(d) R4 ($\Lambda_{avg} = < 0.1$).

Figure 10. - Ferrogram deposit at 54 millimeters for rough ball series.

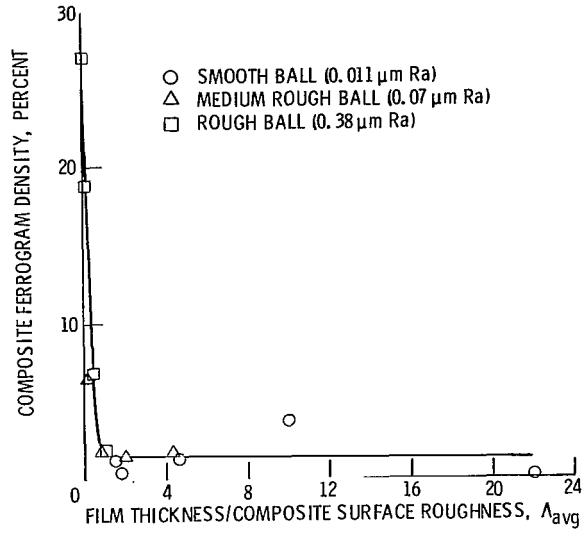

Figure 11. - Composite ferrogram density as a function of Λ_{avg}.

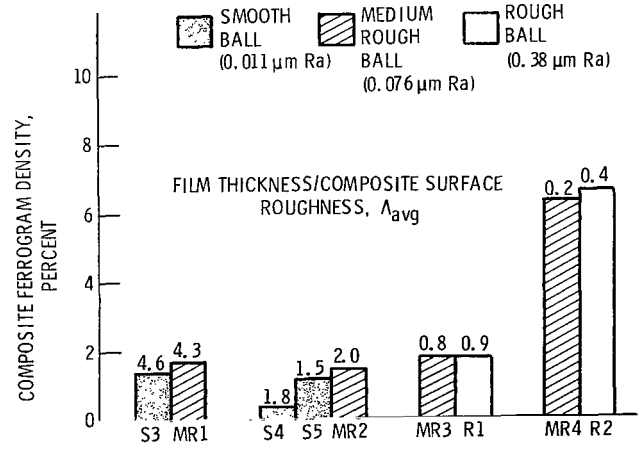

Figure 12. - Comparison of composite Ferrogram densities at similar Λ_{avg} ratios.

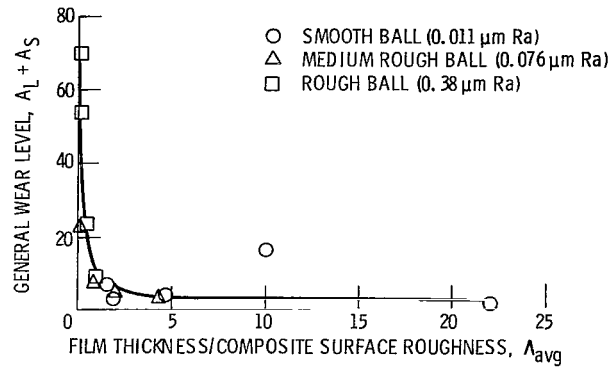

Figure 13. - General wear level ($A_L + A_S$) as a function of Λ_{avg}.

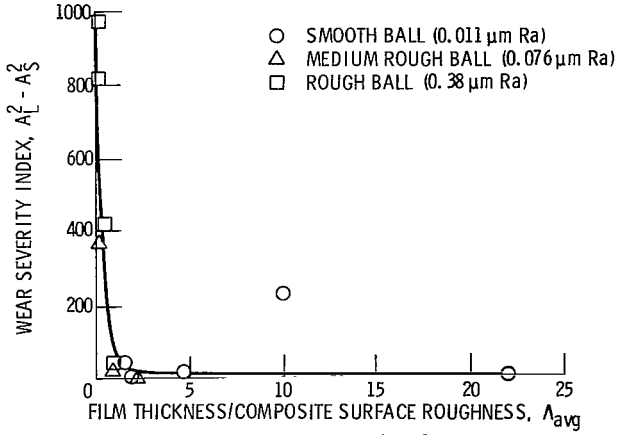

Figure 14. - Wear severity index ($A_L^2 - A_S^2$) as a function of Λ_{avg}.

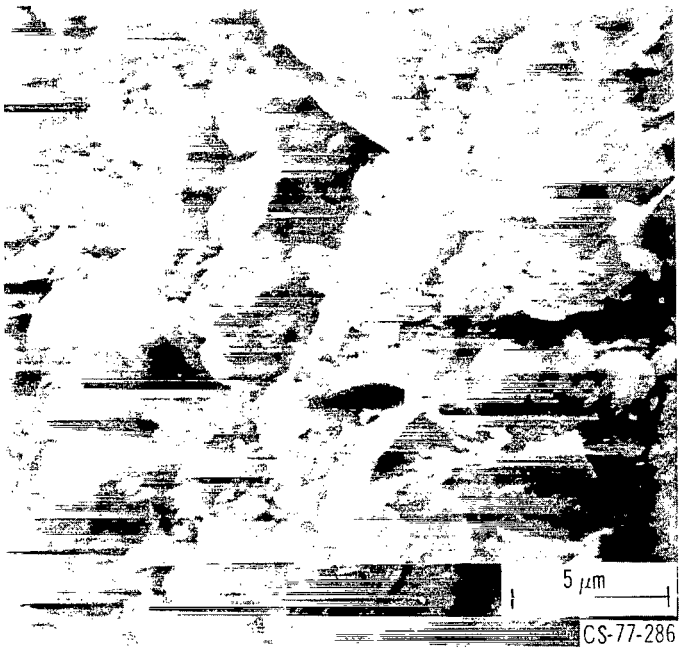

Figure 15. - Normal rubbing wear particles from test R4 (Λ_{avg} <0.1).

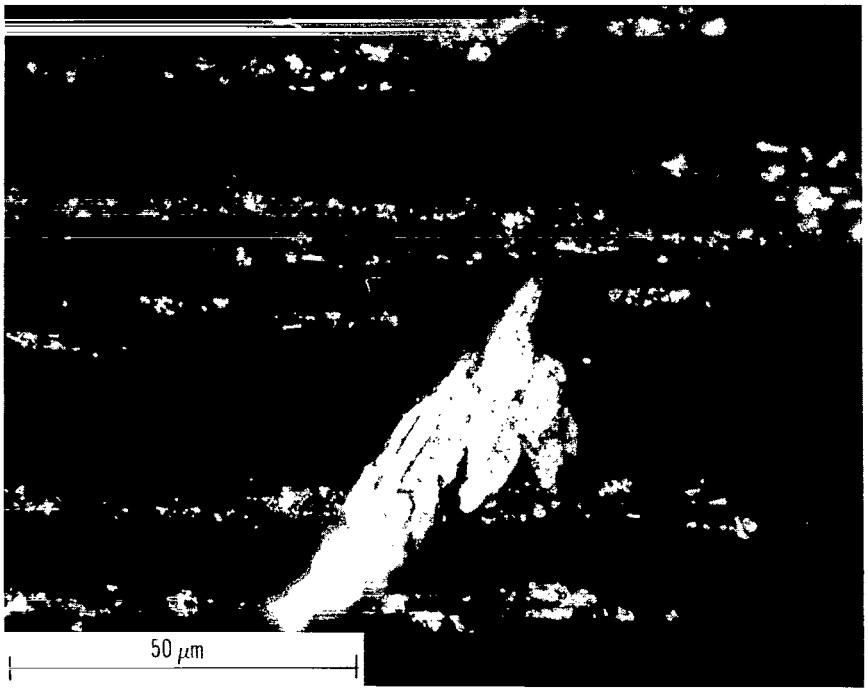

Figure 16. - Aluminum wear particle from test R4.

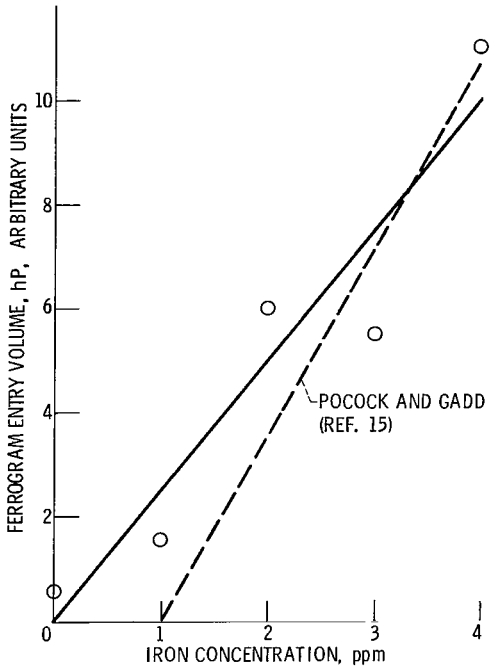

Figure 17. - Ferrogram entry volume as a function of iron concentration in oil.

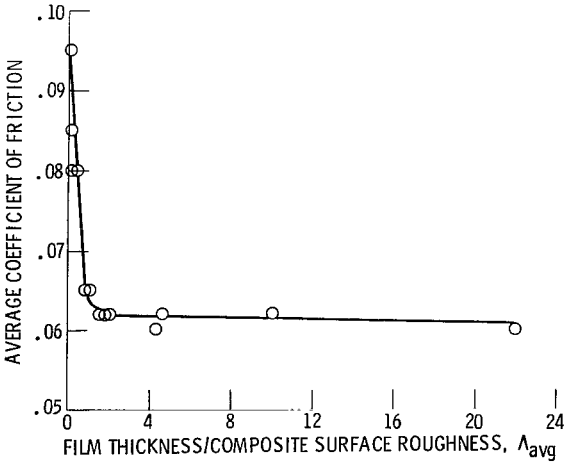

Figure 18. - Average coefficient of friction as a function of Λ_{avg}.

1. Report No.	2. Government Accession No.	3. Recipient's Catalog No.
NASA TP-1230		

4. Title and Subtitle	5. Report Date
FERROGRAPHIC ANALYSIS OF WEAR PARTICLES FROM SLIDING ELASTOHYDRODYNAMIC EXPERIMENTS	April 1978
	6. Performing Organization Code
7. Author(s)	8. Performing Organization Report No.
William R. Jones, Jr., H. S. Nagaraj, and Ward O. Winer	E-9300
	10. Work Unit No.
9. Performing Organization Name and Address	505-04
National Aeronautics and Space Administration Lewis Research Center Cleveland, Ohio 44135	11. Contract or Grant No.
	13. Type of Report and Period Covered
12. Sponsoring Agency Name and Address	Technical Paper
National Aeronautics and Space Administration Washington, D.C. 20546	14. Sponsoring Agency Code

15. Supplementary Notes

16. Abstract

The Ferrograph has been used to analyze wear debris generated in a sliding elastohydrodynamic contact. The amount of wear debris correlates well with the ratio of film thickness to composite surface roughness (Λ ratio). The general wear level parameter and the wear severity index yielded similar correlations with average Λ ratios. Essentially all the generated wear particles were of the normal rubbing wear type. The Ferrograph was more sensitive in detecting the wear debris than was the commonly used emission spectrograph.

17. Key Words (Suggested by Author(s))	18. Distribution Statement
Ferrographic analysis Elastohydrodynamics	Unclassified - unlimited STAR Category 37

19. Security Classif. (of this report)	20. Security Classif. (of this page)	21. No. of Pages	22. Price*
Unclassified	Unclassified	29	A03

* For sale by the National Technical Information Service, Springfield, Virginia 22161

NASA-Langley, 1978

National Aeronautics and
Space Administration

Washington, D.C.
20546

Official Business
Penalty for Private Use, $300

THIRD-CLASS BULK RATE

Postage and Fees Paid
National Aeronautics and
Space Administration
NASA-451

11 1 1U,D, 042078 S00903DS
DEPT OF THE AIR FORCE
AF WEAPONS LABORATORY
ATTN: TECHNICAL LIBRARY (SUL)
KIRTLAND AFB NM 87117

NASA

POSTMASTER: If Undeliverable (Section 158 Postal Manual) Do Not Return